Available online at www.sciencedirect.com
SCIENCE DIRECT®
Journal of Power Sources 139 (2005) 269–273
JOURNAL OF POWER SOURCES
www.elsevier.com/locate/jpowsour

Electrochemical characterization and performance improvement of lithium/sulfur polymer batteries

Xiujian Zhu, Zhaoyin Wen*, Zhonghua Gu, Zuxiang Lin

Shanghai Institute of Ceramics, Chinese Academy of Sciences, 1295 Ding Xi Road, Shanghai 200050, China

Received 23 January 2004; received in revised form 7 May 2004; accepted 14 July 2004
Available online 11 September 2004

Abstract

Electrochemical properties and performance of lithium/polymer electrolyte/composite sulfur cells are presented. The composite sulfur cathode prepared by two ways were characterized and compared by X-ray diffraction (XRD), thermogravimetry (TG), differential thermoanalysis (DTA) and scanning electron microscopy (SEM). The all-solid-state Li/S battery operated at 75 °C with $P(EO)_{20}Li(CF_3SO_2)_2N$–10 wt.%γ-$LiAlO_2$ as electrolyte exhibited an average capacity of 290 mAh g^{-1} for the sulfur melted together with poly(ethylene oxide) (PEO) during 50 cycles. The mechanisms for capacity degradation of the Li/S polymer battery were discussed.

Keywords: Lithium secondary battery; Lithium; Sulfur; Polymer electrolyte; Capacity fade

1. Introduction

The lithium-ion rechargeable batteries have been popularly used in portable electric applications. Based on the purposes to develop lithium batteries for electric vehicles, a battery system with high specific energy, safe operation and low cost would be developed. A lithium/sulfur battery, which use polymer as electrolyte, is expectative due to the theoretical capacity of 1675 mAh g^{-1}, low cost, environment amity of elemental sulfur [1].

Previous reports on Li/S batteries indicated that these problems are incompatibility of lithium and polysulfide with liquid electrolyte, low utilization of sulfur obtained at room temperature, poor cycle performance with aggregation of sulfur after charge–discharge process [1–10]. Shin et al. [7] showed that sulfur of #325mesh particle size was fully utilized for a single discharge at 90 °C and Wang et al. [5,10] reported that the Li/S battery has a high specific capacity value at room temperature when particle size of sulfur less than 10 nm. Consequently, increase of working temperature and reduction of sulfur particle size enhance its utility. Because it is both ionic and electronic insulator, sulfur should be combined well with conductive agent when prepared to electrode. Moreover, the method to prepare composite sulfur cathode is contributing significantly to the electrochemical performance of the Li/S polymer battery.

Solid polymer electrolytes attracted a great deal of interest for using in the Li/S battery, which presented serious defects while liquid electrolyte was employed [8,9]. The poly(ethylene oxide) (PEO) with lithium salts and ceramic filler has been investigated widely during the past decade and has obtained good mechanical properties and ionic conductivity [11–15]. In this work, the PEO with $Li(CF_3SO_2)_2N$ salt and γ-$LiAlO_2$ filler was used as polymer electrolyte for the Li/S battery because of its favorable interfacial stability and electrochemical properties [11–13].

In this paper, we aimed to prepare a stable all-solid-state Li/S polymer battery system and improve its electrochemical performance by developing a new method to prepare composite sulfur cathode.

* Corresponding author. Tel.: +86 21 52411704; fax: +86 21 52413903.
E-mail address: zywen@mail.sic.ac.cn (Z. Wen).

0378-7753/$ – see front matter © 2004 Elsevier B.V. All rights reserved.
doi:10.1016/j.jpowsour.2004.07.002

2. Experimental

2.1. Preparation of composite sulfur cathode and electrolyte

Elemental sulfur (#200mesh) and PEO (M_w = 9 × 10^5) at a weight ratio of 3:7 were blended by two kinds of route to prepare sulfur-based composite materials marked as SPM, which was blended by mechanical milling at room temperature, and SPT, blended by thermal melting at 180 °C in a sealed container. The speed of mechanical milling was 200 rotations per minute for 120 min and a ball-to-powder weight ratio of 20:1 was chosen. To make composite cathode, the mixed slurry of 80 wt.% SPM (or SPT), 10 wt.% acetylene black (AB) and 10 wt.% polyvinylidene fluoride (PVDF) in *N*-methylpyrrolidinone (NMP) was spread uniformly on a thin aluminum foil.

The composite polymer electrolyte of $P(EO)_{20}Li(CF_3SO_2)_2N$–10 wt.%γ-$LiAlO_2$ was prepared in an argon-filled glove box. The stoichiometric mixture of PEO (M_w = 9 × 10^5) and $Li(CF_3SO_2)_2N$ was dissolved in acetonitrile into which γ-$LiAlO_2$ powders were added. The suspension was cast on a Teflon sheet and then heated to evaporate solvent at 50 °C. After evaporation, the electrolyte film was dried under vacuum at 80 °C for 10 h to the remove residual solvent.

2.2. Measurements

All-solid-state Li/S cells were assembled by sandwiching the polymer electrolyte film (360 μm thick) between a lithium foil (200 μm thick) and the composite sulfur cathode (1.5 cm^2 area) in an Ar-filled glove box. The charge and discharge performance of the cells was measured galvanostatically at 0.1 mA cm^{-2} between 1.5 and 3.2 V with a CT2001A cell test instrument (LAND Electronic Co.) at 75 °C. A Solartron Model 1287 Electrochemical Interface was used for cyclic voltammogram measurements. X-ray diffraction (XRD) patterns were recorded using D/max 2550 V XRD spectrometer. Thermogravimetry (TG) and differential thermoanalysis (DTA) were carried out with a ZRY-1P thermal analyzer at the heating rate of 5 °C min^{-1}. The morphology of the electrodes was investigated by scanning electron microscopy (SEM) using a JEOL electronic microscope JSM-6700F.

3. Results and discussion

3.1. XRD and TG/DTA analysis of sulfur composite materials

The fulvous flaky sample of SPT is obtained from a sealed container in which mixture of sulfur and PEO with a weight ratio of 3:7 was melted at 180 °C. Fig. 1 shows the XRD patterns of the sulfur, PEO and SPT. It is clear that the XRD pattern of sulfur shows the characteristic pattern of S_8 and

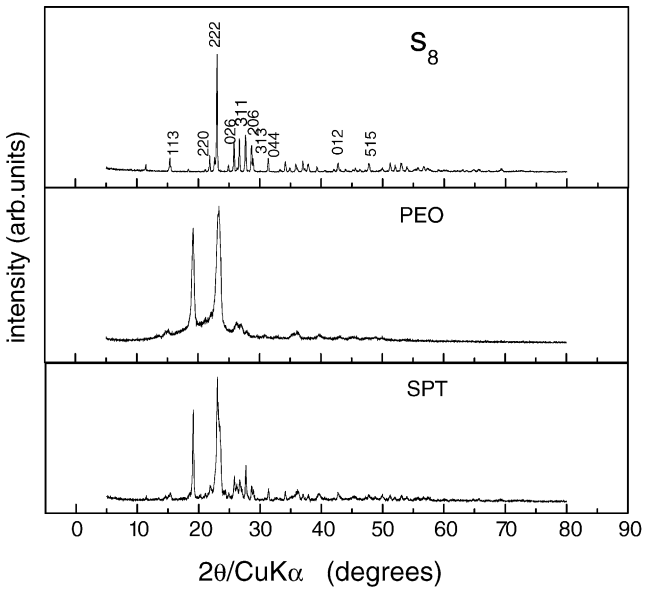

Fig. 1. X-ray diffraction patterns of S_8, PEO and SPT.

conforms to Fddd orthorhombic structure [16,17]. It is therefore suggested on the basis of phase analysis that SPT is only a mixture of sulfur and PEO.

Fig. 2 shows the TG/DTA profiles of SPM and SPT. In the DTA curve, the endothermic peaks around 65 and 120 °C are respectively attributed to the vitrification of PEO and solid–liquid transition of sulfur. In the TG curve, the weigh of the sample shows a drop in the range between 180 and 290 °C. This weigh loss around 30% could be attributed to the volatilization of sulfur, and then the gently decline after 290 °C is corresponding to decomposition of PEO with an exothermic peak in the DTA curve. The TG/DTA patterns of both SPM and SPT are very similar, although the peak temperature of SPT shifts to higher temperature compared to that of SPM.

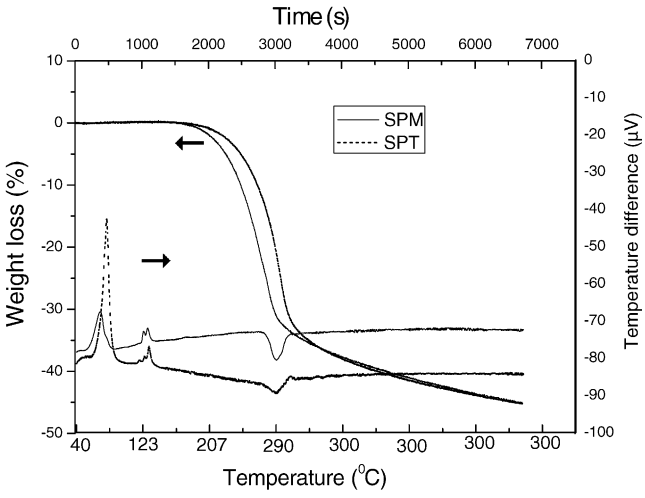

Fig. 2. TG/DTA curves of the SPM and the SPT at a heating rate of 5 °C/min from 40 to 300 °C and then kept at 300 °C under N_2 atmosphere.

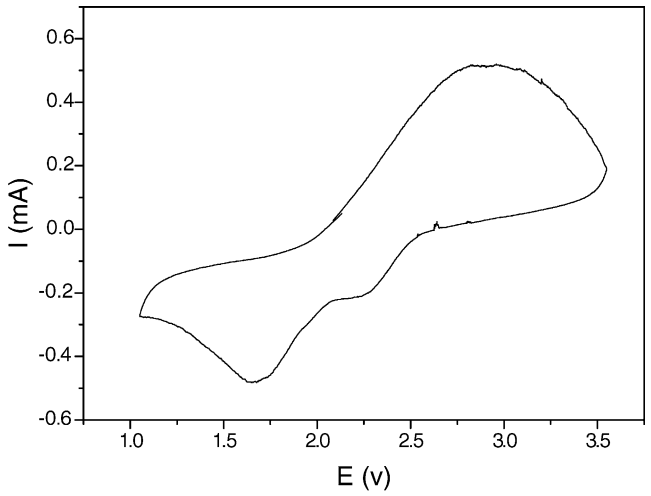

Fig. 3. Cycle voltammograms of Li/SPM polymer cell with sweep rate of 0.5 mV s^{-1} at 75 °C.

Although SPM and SPT have the same compositions, their binding strengths between PEO and sulfur seem very different. The charge–discharge performance of cells is investigated as follows.

3.2. Electrochemical properties of Li/S polymer batteries

Cyclic voltammograms for the Li/SPM polymer cells after 10 cycles given in Fig. 3 are more or less similar to the results obtained by Jeon et al. [6]. The reduction of sulfur occurs in two steps: the first around 2.3 V is for polysulfide to short lithium polysulfide (Li_2S_n, $2 < n < 8$), and the second around 1.7 V is for further reduction to lithium sulfide (Li_2S, Li_2S_2) [1,6].

It was reported that the lithium ionic conductivity of PEO–LiX electrolyte with γ-$LiAlO_2$ filler is above 10^{-4} S cm^{-1} at the temperature higher than the vitrification point (65 °C) of PEO.[13] Therefore, different from Marmorstein' s work in which PEO was used as electrolyte and operated up to 90 °C to achieve satisfactory conductivity [1], Li/S battery with $P(EO)_{20}Li(CF_3SO_2)_2N$–10 wt.%γ-$LiAlO_2$ as electrolyte could operated at 75 °C, so that the electrolyte film demonstrated favorable stability to reach a longer cycling life. It is known that the $Li(CF_3SO_2)_2N$ is one of the most reactive salts causing corrosion of aluminum current collector in organic solvent electrolyte and has a pitting potential of 3.55 V versus Li/Li^+ at aluminum [19–21]. Although the $Li(CF_3SO_2)_2N$ used here in all solid polymer system may diffuse to cathode during cycling, the corrosion of aluminum was not observed in our experiment after 50 cycles where the cycling window was in the voltage range of 1.5–3.0 V, which demonstrated that at a potential lower than the pitting potential of $Li(CF_3SO_2)_2N$ at aluminum, the corrosion would be negligible.

The charge and discharge voltage profiles for selected cycles of the Li/SPM (or SPT) polymer cells are shown in Fig. 4. It is obvious that the discharge plateau of the cell falls gradually from 2.1 to 1.9 V after 10 cycles with the increasing of the charge plateau and fades at the 50th discharge. The enlarged gap between charge plateau and discharge plateau may be due to the increase of resistance attributed to the formation of large particles of highly resistive sulfur or lithium sulfide. Compared to the charge–discharge plateau of the Li/SPM cell, the charge–discharge plateau of the Li/SPT cell keeps

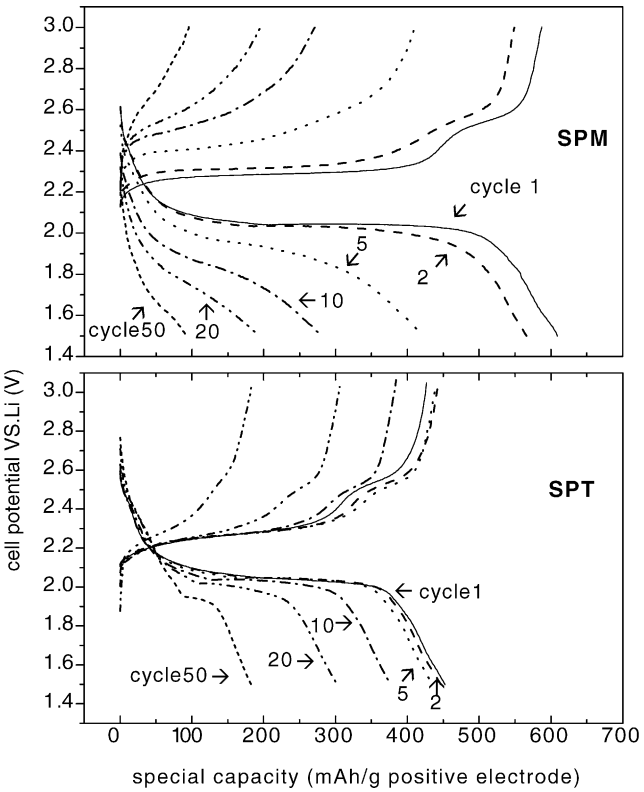

Fig. 4. Typical charge–discharge curves of a Li/SPM cell (upper) and a Li/SPT cell (lower) at 0.1 mA cm^{-2} and 75 °C within 1.5–3.0 V potential cutoff window.

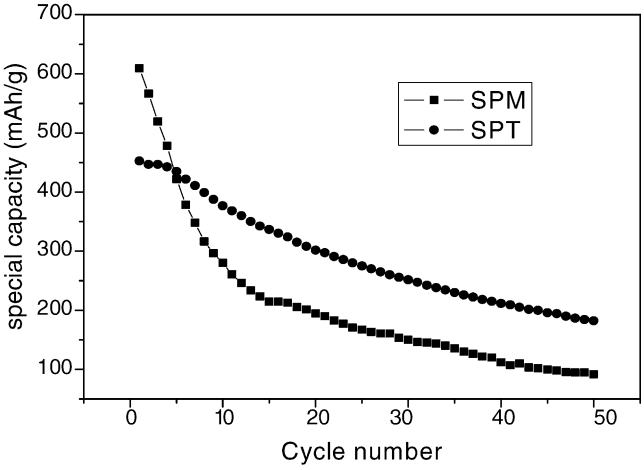

Fig. 5. Comparison of cycle life of Li/SPM cell vs. Li/SPT cell discharged to 1.5 V cutoff (0.1 mA cm^{-2} and 75 °C).

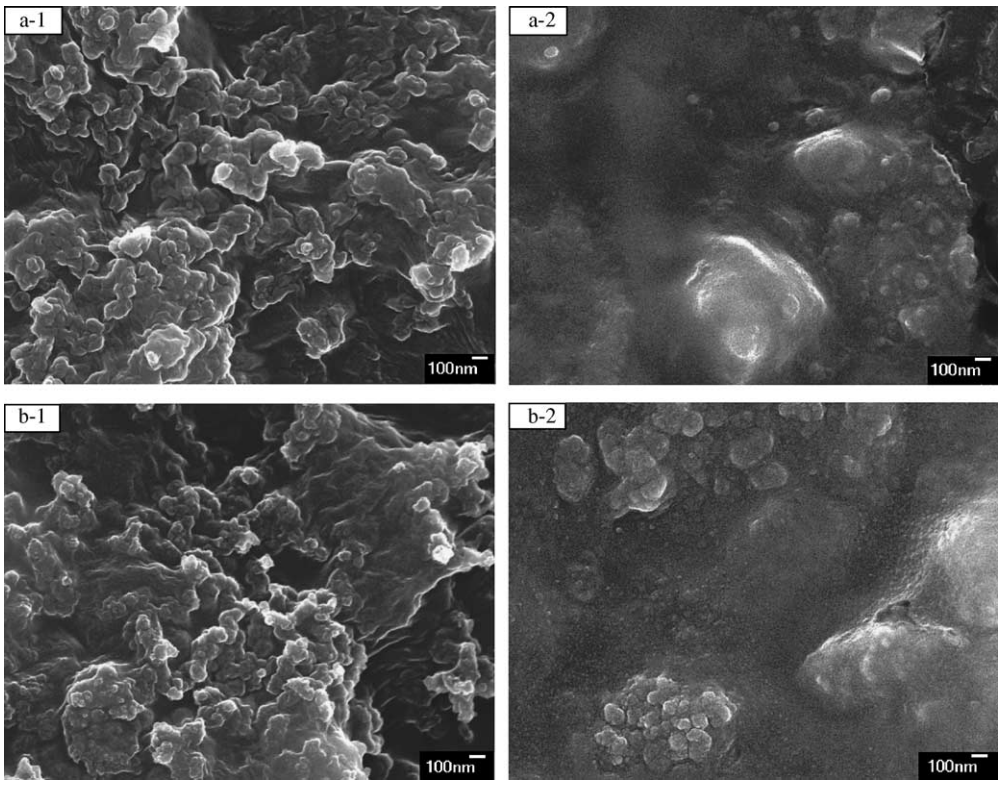

Fig. 6. SEM photographs of composite cathode: (a-1) SPM as prepared and (a-2) after 50 cycles; (b-1) SPT as prepared and (b-2) after 50 cycles.

well from the first to the 10th cycle and is still clear at the 50th cycle.

The capacity fade of Li/SPM (or SPT) cells is given in Fig. 5. The discharge capacity of Li/SPM cell is 609 mAh g^{-1} at the initial cycle but fades quickly to 280 mAh g^{-1} after the first 10 cycles and then declines slowly to 91 mAh g^{-1} at the 50th cycle. The cycling performance of Li/SPM cell is similar to the results reported previously by Marmorstein et al. [1] and Shin et al. [7]. The Li/SPT cell has discharge capacities of 452 and 184 mAh g^{-1} at the first and 50th discharge, with an average fading rate of 5 mAh g^{-1} per cycle in 50 cycles, which is much lower than Li/SPM cell.

Jeon et al. [6,18] suggested that high capacity fading rate for composite sulfur electrode is mainly due to the heterogeneity and worsen distribution of sulfur along with cycling. In our work, morphology of SPM and SPT cathode were also investigated.

3.3. Morphology of composite cathode in Li/S polymer batteries

The morphology of composite cathode observed by field emission SEM with 3×10^4 magnification is shown in Fig. 6. As seen in figures a-1 and b-1, both SPM and SPT cathode displayed homogeneous distribution of sulfur in PEO matrix before charge–discharge cycling. The sulfur with particle size about 100 nm in diameter is well enwrapped by PEO. However, after 50 cycles experiment, sulfur particles do not remain their original positions in PEO and heterogeneous distribution of sulfur component was presented as demonstrated in figures a-2 and b-2 for SPM and SPT respectively. Such morphological feature was in accordance with the results reported by other research group [6,18]. A reasonable explanation for the high capacity fading rate therefore could be suggested, i.e., the loss of electrical contact during cycling is mainly due to the aggregation of sulfur or lithium sulfide. Although it is difficult to discern which one was more seriously aggregated from SEM photographs between SPM and SPT cathode as shown in a-2 and b-2, the improved cycling-stability of the cell with SPT cathode is likely related to the prohibited aggregation process of the sulfur in the PEO matrix during charge–discharge cycling.

4. Conclusions

The all-solid-state Li/S cell with $P(EO)_{20}Li(CF_3SO_2)_2N$–10 wt.%γ-$LiAlO_2$ as electrolyte operates at 75 °C exhibit an average capacity of 290 mAh g^{-1} in 50 cycles. The cycle-stability of Li/S polymer battery can be improved by amending the method to prepare the PEO_S composite cathode. The capacity of Li/S polymer battery is mostly suffered from aggregation of sulfur or lithium sulfide during cycling.

Acknowledgments

This work was financially supported by key project of Natural Science Foundation of China (NSFC) No. 20333040.

References

[1] D. Marmorstein, T.H. Yu, K.A. Striebel, F.R. McLarnon, J. Hou, E.J. Cairns, J. Power Sources 89 (2000) 219–226.
[2] Y.M. Lee, N.S. Choi, J.H. Park, J.K. Park, J. Power Sources 119–121 (2003) 964–972.
[3] B. Jin, J.U. Kim, H.B. Gu, J. Power Sources 117 (2003) 148–152.
[4] A. Hayashi, T. Ohtomo, F. Mizuno, K. Tadanaga, M. Tatsumisago, Electrochem. Commun. 5 (2003) 701–705.
[5] J.L. Wang, L. Liu, Z.J. Ling, J. Yang, C.R. Wan, C.Y. Jiang, Electrochim. Acta 48 (2003) 1861–1867.
[6] B.H. Jeon, J.H. Yeon, K.M. Kim, I.J. Chung, J. Power Sources 109 (2002) 89–97.
[7] J.H. Shin, K.W. Kim, H.J. Ahn, J.H. Ahn, Mater. Sci. Eng. B 95 (2002) 148–156.
[8] H. Yamin, A. Gorenshtein, J. Penciner, Y. Sterberg, E. Peled, J. Electrochem. Soc. 135 (1988) 1045–1048.
[9] E. Peled, Y. Sternberg, A. Gorenshtein, Y. Lavi, J. Electrochem. Soc. 136 (1989) 1621–1625.
[10] J.L. Wang, J. Yang, C.R. Wan, K. Du, J.Y. Xie, N.X. Xu, Adv. Funct. Mater. 13 (2003) 487–492.
[11] Z.Y. Wen, T. Itoh, M. Ikeda, N. Hirata, M. Kubo, O. Yamamoto, J. Power Sources 90 (2000) 20–26.
[12] Z.Y. Wen, T. Itoh, Y. Ichikawa, M. Kubo, O. Yamamoto, Solid State Ionics 134 (2000) 281–289.
[13] F. Croce, L. Persi, F. Ronci, B. Scrosati, Solid State Ionics 135 (2000) 47–52.
[14] R. Oesten, U. Heider, M. Schmidt, Solid State Ionics 148 (2002) 391–397.
[15] F.R. Kalhammer, Solid State Ionics 135 (2000) 315–323.
[16] C. Gallacrer, A.A. Pinkerton, Acta Cryst. C49 (1993) 125–126.
[17] J. Rettig, J. Trotter, Acta Cryst. C43 (1987) 2260–2262.
[18] B.H. Jeon, J.H. Yeon, I.J. Chung, J. Mater. Process. Technol. 143–144 (2003) 93–97.
[19] L.J. Krause, W. Lamanna, J. Summerfield, M. Engle, G. Korba, R. Loch, R. Atanasoski, J. Power Sources 68 (1997) 320–325.
[20] W.K. Behl, E.J. Plichta, J. Power Sources 72 (1998) 132–135.
[21] B. Garcia, M. Armand, J. Power Sources 132 (2004) 206–208.